The nanostructure of surfactant-DNA complexes with different arrangements†

Amalia Mezei[1], Ramon Pons[1*], M. Carmen Morán[2]

Abstract

The nanostructure of DNA with different cationic surfactant has been studied in order to elucidate the detailed arrangement concerning the position of DNA and surfactant domains in the complexes. Also, the orientation of the DNA cylinders in the thin films of the complexes was investigated. Attention was directed on the preparation methods of the complexes and to how the different surfactant structure affects the compaction of the DNA. The cationic surfactant-DNA complexes were investigated by X-ray scattering, Polarized light Microscopy and Elemental Microanalysis. It was observed that the molecular organization of the complexes between DNA and cationic surfactant correspond to a hexagonal structure with different packing arrangements. The nanostructure of the complexes depends on the hydrophobic/hydrophilic balance of the cationic surfactant. In particular the use of arginine derived surfactants, with a large polar head group able to interact not only by electrostatics but also by hydrogen bonding, allows for the formation of more compact structures. The results suggest that the smaller the lattice parameter the more compact and stable is the complex implying slower DNA release.

1. Introduction

The development and the study of the nanostructure of DNA derivatives are a fundamental achievement in the field of biomaterials for pharmaceutical applications. It is well known that naturally derived polyanions such as nucleic acids (DNA and RNA) can self-assemble with cationic lipids or surfactants via electrostatic attractions, thermodynamically driven by the release of counterions.[1] Applications of these types of complexes are frequently used in the fields of pharmaceuticals and gene delivery.[2, 3] Most of these complexes are dispersed in aqueous solution with well understood characterized structures.[2,3, 4] The interaction between oppositely charge amphiphiles and macromolecules has also relevance in biological systems. For instance, in gene transfection the reversible collapse and swelling of DNA molecules are required. This behavior can be achieved by subsequent complexation of DNA with cationic surfactants.[5] The DNA condensation has received considerable attention in recent years due to its biological importance in DNA packaging in virus heads, as well as, in the development of gene delivery vehicles.[6,7,8] Multivalent metal cations and positively charged polymers, such as polyamines or peptides are known to provoke the condensation of DNA to particles that appear as rods, toroids or spheroids under the electron

[1]Departament de Tecnología Química y de Tensioactius, Institut de Química Avançada de Catalunya, IQAC-CSIC, c. Jordi Girona 18-26, 08034 Barcelona, Spain, Tel:+34 93 4006150, Fax: +34 93 2045904

[2]Departament de Fisiología, Facultat de Farmàcia, Universitat de Barcelona, Avda. Joan XXIII, 08028 Barcelona, Spain, Tel: +34 93 402 1093, Fax: +34 93 403 1886

[*]Corresponding author e-mail: *ramon.pons@iqac.csic.es*

†Electronic supplementary information (ESI) available: The three different preparation methods and for ALA-DNA an experimental and simulated azimuthal scattering spectra.

microscope. It was shown that the oppositely charged polyelectrolytes, such as the proteins, lysozyme and protamine sulfate, are very efficient compaction agents.[9] The conformational behavior of DNA in the presence of proteins follows a discrete transition between expanded coil and condensed globule, with a coil-globule coexistence region. Pinto et. al [10] showed that it is possible to obtain a variety of conformations, degrees of compaction and aggregation simply by controlling the way DNA comes into contact with the condensing agent.

The mixtures of DNA and cationic surface active molecules constitute the basis of formulating DNA. For this reason, it is evident the need for a better understanding of the structures formed and of the interactions in mixed systems of DNA and surfactants. For uses in the biomedicinal field, biocompatibility and biodegradability of the vehicle molecules is needed.[11] Among the possible surfactant candidates, the amino acid derived surfactants are a family of choice, because of good biocompatibility. Therefore, these surfactants are of great interest in the field of novel non viral drug delivery devices.[12,13,14] Up to now it has been found that the complex structure (such as lamellar, inverted hexagonal or hexagonal) mainly depends on the lipid used for complexation.[15, 16] However, the results, in term of nanostructure of the complexes are not clear. The reasons are the orientation of DNA domains and surfactant conformation. Because non equilibrium structures strongly depend on the preparation method it is important the knowledge of the mixing protocols, for instance a simple preparation of cationic surfactant-DNA films or gel particles was previously reported.[17,18] Nanoparticles formed from oppositely charged polymers and surfactants might display different structures and compositions. The number of applications proposed for nanoparticles is constantly increasing, being reflected in a particularly prominent number of papers and patents, as well as formulations undergoing clinical trials. It is frequently observed the application in the pharmaceutical area, the list of commercially available products becomes very narrow, mainly because of regulatory hurdles to demonstrate their safety for human use.

The difficulties encountered with the nanostructural control in the complexes have motivated attempts to prepare well-ordered films/particles. Recent studies indicate the formation of a columnar hexagonal liquid crystalline packing of DNA in the presence of polyamines and other multivalent cations.[19] X-ray diffraction studies of DNA-lipid/surfactant systems have shown the presence of organized structures, mainly liquid crystalline in nature.[1,20] However, little is known about the behavior of the complexes at microstructure level. The aim of this work is to clarify the hexagonal-lamellar structure of the surfactant-DNA complexes and also to clarify the orientation of DNA domain in thin films. This last point has relevance because the dry films or coatings may have distinct advantages for drug or nucleic acid delivery such as direct implantation at the site interest, direct storage capabilities, ease of handling, etc. The drug release behavior and catalytic activity of these nanoparticles are strongly influenced by their morphology. The size will affect the level of cellular uptake of the drug, the thickness and porosity the drug transport

efficiency, and the drug loading concentration the release rate. The drug delivery application of DNA nanomaterials includes the collapse of extended DNA chains into compact, orderly particles containing only one or few molecules.[21,22] For these reasons, the study of microstructure of these complexes has an up to date importance.

In this paper, we present a systematic investigation of the dry films prepared by different methods by X-ray scattering, polarized light microscopy and elemental microanalysis. The general nanostructure of cationic surfactant-DNA complexes will be discussed and also potential practical applications of the results will be suggested.

2. Experimental Section

2.1 Materials

The sodium salt of deoxyribonucleic acid (DNA) from salmon testes of an average degree of polymerization of about 2000 base pairs was purchased from Sigma-Aldrich and used as received. The DNA concentrations were determined spectrophotometrically (assuming that, for an absorbance of 1 at 260 nm, a solution of DNA has a concentration of 50 μg/mL).[23]

Cetyltrimethylammonium bromide - CTAB, myristyltrimethylammonium bromide - MTAB and sodium bromide - NaBr were obtained from Sigma-Aldrich. The arginine-N-lauroyl amide dihydrochloride (ALA) and N^{α}-lauroylarginine-methyl ester hydrochloride (LAM) were synthesized in our laboratory.[24,25]

All experiments were performed in 10 mM NaBr solutions, using Millipore Milli-Q deionized water.

(a)

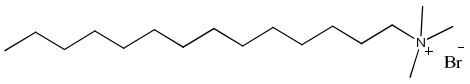

(b)

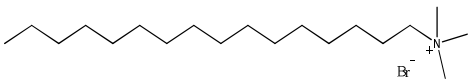

(c)

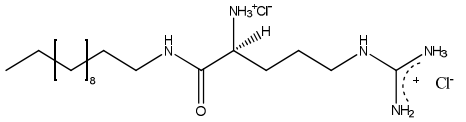

(d)

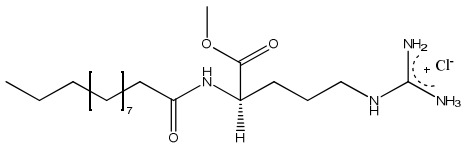

Figure 1: Chemical structure of the studied cationic surfactants. a.) Myristyl-trimethylammonium bromide– MTAB b.) Cetyl-trimethylammonium bromide – CTAB, c.) Arginine-N-lauroyl amide dihydrochloride – ALA and d.) N^{α}-lauroyl-arginine-methyl ester hydrochloride – LAM

2.2 Sample Preparation

DNA stock solutions were prepared in 10 mM NaBr to stabilize the DNA secondary structure in its native B-form conformation. The surfactants were also dissolved in 10 mM NaBr. Particles or films were prepared at defined ratio R, where R = [DNA]/[S^+], where [S^+] is the concentration of the corresponding surfactant system. In the case of ALA [S^+] is the equivalent surfactant concentration, taking in account the positive charges in the molecule. In all cases, [DNA] was equal to 2 % (w/v) and the surfactant concentration was also 2 % (w/v), which for all of them, results in concentrations, around 60 mM. Using the stock solution of DNA and of surfactants three types of sample preparation were applied (Figure 1S in Supplementary Information):

Method 1 - *Particle formation*, DNA solutions were added drop wise into gentle agitated surfactant solutions. After 2h, the formed particles were separated by filtration from surfactant solution and washed with water, to remove the excess of surfactant and salt. For measurements the particles were open with a needle and fixed on a flat glass surface;

Method 2 - *Film formation* on a flat surface, the DNA and surfactant solution were simultaneously sprayed on flat glass surface.

Method 3 - *Film formation in capillaries*, first the DNA solution was introduced in the capillary and then slowly the surfactant solution was added, after few seconds at the interface of the two solutions the film formation was observed.

2.3 Polarized Light Microscopy (PLM)

A Zeiss polarized light microscope equipped with a Linkam LTS120 hot stage, controlled by PE94 unit was used. Images were acquired with a Canon PowerShot S90 Wide Zoom digital camera. Anisotropic liquid – crystalline phases give rise to typical birefringent textures under polarized light.

2.4 Small Angle X-ray Scattering (SAXS) and Grazing Incidence SAXS (GISAXS)

Small Angle X-ray measurements were carried out using a S3-MICRO (Hecus X-ray systems GMBH Graz, Austria) coupled to a GENIX-Fox 3D X-ray source (Xenocs, Grenoble), which provides a detector focussed X-ray beam with the Cu Kα-line (wavelength 1.542 Å) with more than 97% purity and less than 0.3% Kα. Transmitted scattering was detected using a PSD 50 Hecus in 1D experiments with a pixel resolution of 54.2 μm and approximately 1 cm pixel width and a CCD Gemstar (Microphotonics Inc.) for

the 2D images with a pixel size of 28.6 x 28.6 μm^2. Temperature was controlled by a Peltier TCCS-3 Hecus model working with ±0.1 ^{o}C resolution.

For the X-ray measurements, the gel particles and the films were dried. All the measurements were done at room temperature under vacuum. The dry surfactant powders were inserted in a glass capillary 1 mm diameter with 20 μm wall thickness. The surfactant-DNA films were deposited on glass-plate.

The SAXS scattering curves are shown as a function of the scattering vector modulus,

$$q = \frac{4\pi}{\lambda} sin\ \frac{\theta}{2}$$

where θ is the scattering angle and λ the wavelength of the radiation. The q range obtained with our setup was between 0.08 – 6 nm^{-1} in the SAXS regime.[26] The system scattering vector was calibrated by measuring a standard silver behenate sample. The scattering curves show mainly slit-length smearing because of the use of a detector focused small beam (300 x 400 μm full width at half maximum). This mainly produces a widening of the peaks without a noticeable effect on the peak position. The instrumentally smeared experimental SAXS curves were fitted to numerically smeared models for beam size and detector width effects.

In the GISAXS configuration, the samples were deposited on glass plates. The samples were oriented with respect to the incident beam using a high-resolution stepper motor. The angle was kept between 0.5 and 0.8 degree. The 2D images were analyzed with FIT2D software to obtain the one-dimensional spectra or radial cuts.

3. Results and discussion

3.1. Observations related to sample preparation

In order to clarify the nanostructure of cationic surfactant-DNA complexes, in this work three different methods were studied for the complex/film production. Several aspects inherent to the preparation procedure will be mentioned that affects the final properties of the particles. In a recent study[27] in which we produced cationic surfactant-DNA gel particles, it was observed that a positive/negative charge ratio around 1 resulted in the formation of particles. The main purpose of this work was to investigate the nanostructure of cationic surfactant-DNA materials and lead to new insight into how drug delivery systems can be designed on the basis of appropriate phase behavior.

The structure and properties of the studied complexes in thin film geometry can be significantly different from the bulk properties. The presence of two interfaces, the air-film interface and film-substrate

interface, can induce preferential ordering in the films, in particular, if the film thickness is of the order of the typical length scale of the macromolecule microstructure.

The direct association of cationic surfactant to DNA decreases the effective charge of the nucleic acid, allowing the surfactant-DNA complex to form a membrane. DNA gel particles and DNA films were prepared using solutions with a concentration such that R = 1. The formation and the stabilization of the DNA gel particles were earlier studied[24, 18] using mixtures of DNA and cationic surfactants. In this work, the nanostructure of the obtained translucent, gel particles were studied in detail, in particular in the form of stable cationic surfactant-DNA films.

The studied DNA gel particles were obtained by mixing double stranded DNA with single chain cationic surfactants. The structure of the latter differs in hydrophobic chain length and also in the hydrophilic head group. The polar/hydrophobic character of the counter-ion, as earlier studies show, have an important role in the final properties of the particles obtained[28]. The studies were carried out on films obtained from the different methods (please refer to the above section 2.2 for more details on the preparation methods). The thicknesses of those films were between 1-2 mm and they showed an opaque structure. Measurements were carried out on dry films in vacuum.

3.2 Lyotropic Properties by Polarized Light Microscopy

The phases formed by DNA and cationic surfactant complexes can be identified initially using polarized light microscopy (PLM). All complexes were found to be birefringent under the polarized light. The qualitative phase behavior of the materials was observed by microscopy, and the obtained results are presented in Figure 2. The first observation was the different texture of these complexes. Not clearly defined structures were observed. However, for the samples prepared by the different methods the coexistence of lamellar or hexagonal structure was mainly detected.

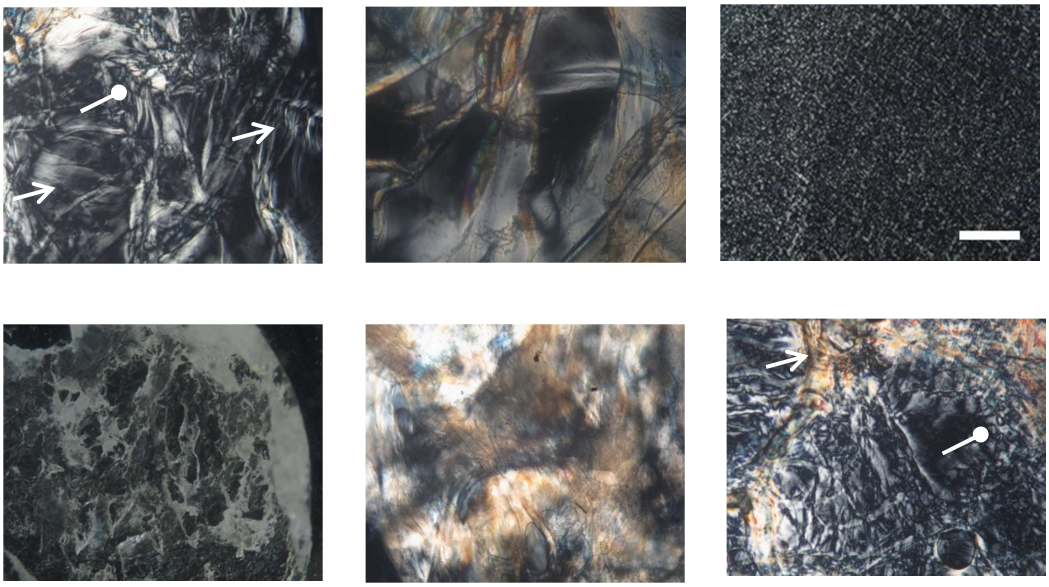

Figure 2: Representative optical polarized display micrographs for surfactant-DNA complexes at 25 ^{o}C using different methods: a), b), d) and e) are DNA films obtained using method 1 and opening the corresponding particle; c) and f) are DNA films obtained using method 2 obtained by spraying method. The scale bar shown in c) is valid for all the micrographs and corresponds to 50 μm. → point to lamellar and ⊣● to hexagonal textures.

The PLM image in Figure 2 exhibits the coexistence of crossed textures and veins, which are typical texture for the lamellar (L_{α}) phase and some "fan" pattern for the hexagonal lattice (H).[29] The textures formed by CTAB-DNA, MTAB-DNA, LAM-DNA from the appearance of the optical texture can readily be identified as a lamellar liquid-crystalline phase by its characteristic texture. For ALA-DNA, not very defined structure was observed. The appearance of the smoky texture and the presence of spherulites suggest a hexagonal structure[29]. Surfactant-DNA complexes additionally form some birefringent crystals with sharp edges, by method 2 (dry film by spraying method). These crystals might be ascribed to varying sample thickness and the contact time of the two solutions. For all investigated complexes, it was found reproducibly that the birefringent texture of the films changes gradually with the thickness of these films.

3.3 X-ray scattering studies

3.2.1. SAXS Studies

Further insight into the structural properties of the constituent phases of the different formulations was obtained by using X-ray scattering measurements (SAXS and GISAXS). As it is well known SAXS intensities are Fourier transforms of the correlation function, which in turn is a product of the form factor and the structure (interference) factor.

For a systematic study first the dry powder of the corresponding surfactants were measured in a glass capillary (with 1 mm diameter) at 25±0.1°C. The SAXS spectra of the surfactants are presented in Figure 3. The small-angle X-ray diffraction pattern showed a series of reflection peaks characteristic of lamellar packing for each surfactant.

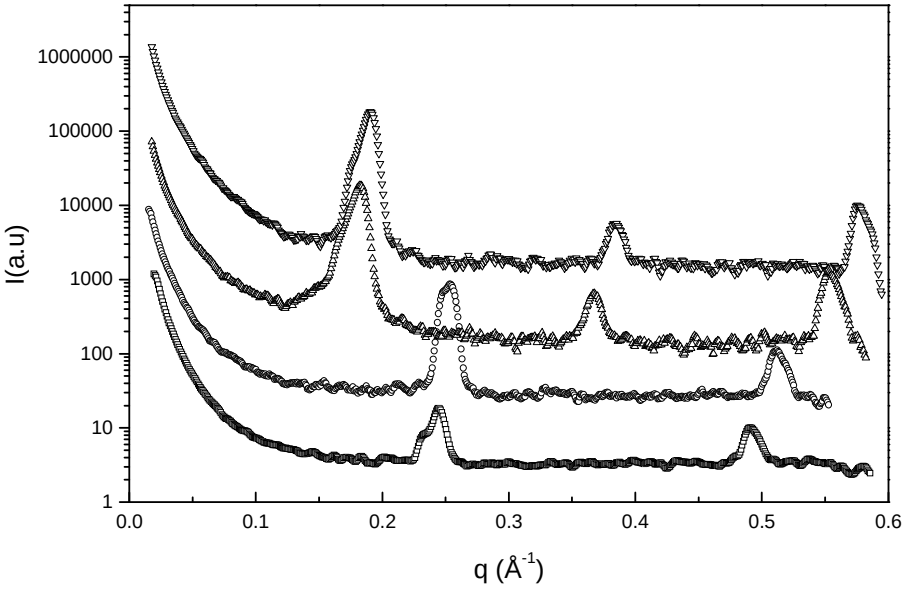

Figure 3: SAXS spectrums of the studied dry surfactant powder at room temperature (25±0.1°C). In order, from bottom to top: CTAB (□), MTAB (○), ALA (Δ) and LAM (∇). The curves have been smoothed by adjacent averaging of 5 points.

The X-ray patterns consist of two or three peaks in the small angle scattering vector *q* in the ratio 1: 2: 3. Further, all Bragg peaks have similar profiles. The intermolecular distance is changing with the hydrocarbon chain length, and this can be observed in the position of the last peak in the spectra. The first maximum in the scattering intensity will be treated as a lamellar peak. Table 1 summarizes the position of the first Bragg-reflection, the corresponding morphology, and it's *d*-spacing. For CTAB and MTAB surfactants (16 and 14 carbon atoms in the hydrocarbon chain), the parameters are smaller compared to the arginine–derivatives with 12 carbon atoms in the hydrocarbon chain. The SAXS studies show that, for the surfactants with 12 carbon atoms in the hydrocarbon chain, the repeating distance is 34.5 and 32.9 Å for ALA and LAM respectively. The structure of ALA and LAM surfactants differs mainly on the connection of the alkyl chain to the carboxyl group (ALA) or to α amino group (LAM) of arginine (see Figure 1), and the repeating distance is not changing significantly. In the case of MTAB and CTAB, an alteration of the hydrophobic chain length can be observed in the packing[30], as the hydrophilic part of the molecules contain a bromide, the molecules pack as a repeating double layer and the hydrophobic chain

are tilted with respect to the basal plane. In addition, it was shown by Paradies et al.[31] that different conformation can be observed depending on the CTAB crystals growth conditions within a narrow range of physical parameters including the application of organic solvent. Different polymorphs were obtained where the CTAB molecules were packing in a bilayer, and the Br^- anions were located at different positions in the three CTAB polymorphs with respect to the extended n-alkyl chains (around 0.4 nm far away from the quaternary nitrogen). The widely different repeating distances for the quaternary ammonium salts (as compared to the lipoaminoacids) are a reflection of the different structure of the polar heads which affects also the hydrocarbon chain packing. It is clear that the preferred structure has to be much more extended in the latter than in the former.

Table 1: SAXS characterization of the studied surfactants

Dry surfactant	q_{max} ($Å^{-1}$)	Morphology	d (nm)
CTAB	0.244	Lamellar	2.57
MTAB	0.254	Lamellar	2.49
ALA	0.182	Lamellar	3.45
LAM	0.191	Lamellar	3.29

Furthermore, the nanostructure of the surfactant-DNA complexes was studied in dry conditions. The dry films of surfactant-DNA complexes were investigated by SAXS and GISAXS measurements. For CTAB-DNA, MTAB-DNA, ALA-DNA and LAM-DNA complexes, the structure is manifestly different to that of the dry surfactant. In Figure 4 SAXS spectra of Cationic surfactant-DNA films obtained using the three different preparation methods are shown.

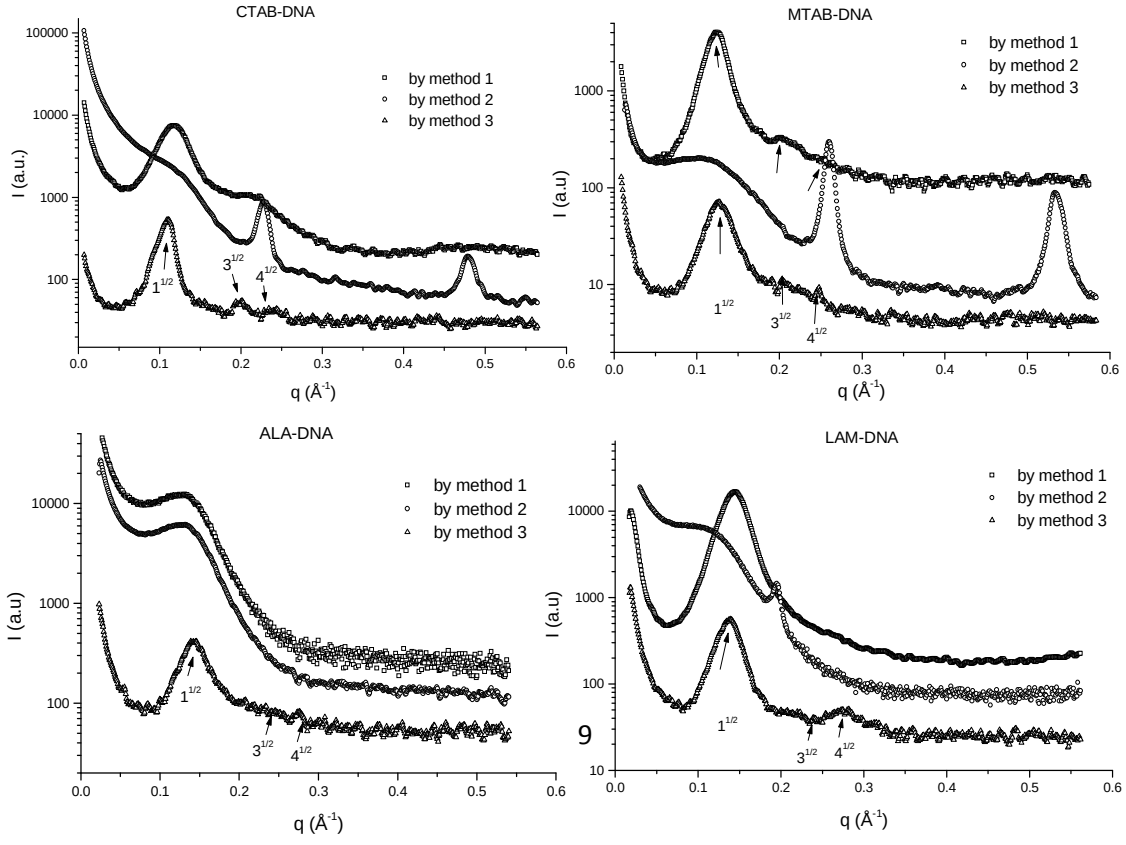

Figure 4: SAXS spectra for Cationic surfactant-DNA films obtained using the different preparation methods at room temperature (25±0.1°C). The spectra are shown from top to bottom: Method 1 (□) Method 2 (○) and Method 3 (Δ). The curves have been smoothed by adjacent averaging of 5 points. The small arrows show the approximate position of the hexagonal lattice peaks.

The SAXS spectra for the CTAB-DNA film obtained using method 1 (opening the DNA gel particle) and method 3 (in capillary at the interface) are very similar. A hexagonal packing of rod-like particles should produce scattering pattern with peaks in a 1:√3:2 order. The absence of a second and/or the third peak from a hexagonal structure can be due to the occurrence of minima of the scattering form factor close to the expected reflections as shown by Krishnaswamy et al.[32] Preferred orientation of the rods perpendicular to the film normal would hinder the observation of the √3 peak. The X-ray measurements show a relatively broad peak with a maximum in the range of q=1.1-1.8 nm^{-1}. In the SAXS spectra of Cationic surfactant-DNA film prepared by method 2 (dry film by spraying method), two additional sharp peaks can be seen. These peaks correspond to the 1st and 2nd peak of the dry surfactant, which can be explained by the fact that, in this method, the contact-time of the DNA and surfactant solution is very short, promoting a smaller amount of surfactant-DNA complex in comparison of that formed using the method 3 (in capillary at the interface). The representative SAXS spectra of MTAB-DNA, ALA-DNA and LAM-DNA films, obtained using the different preparation methods, clarify that the structure of the complexes formed by method 1 and 3 is very similar and can be ascribed to a hexagonal packing.

Table 2 shows the corresponding lattice parameters and the repeat distance obtained for the different surfactant-DNA complexes. The peak of the corresponding surfactant-DNA complex has the same position, indifferent from the applying method. This is a bit surprising taking into account that the complex prepared by method 1 is measured in the dry state (vacuum) while the complex prepared by method 3 is measured *in situ*. The consequence of this observation is that the formation of the complex produces a complete or nearly complete dehydration. According to the peak positions of complexes and taking into account a hexagonal packing we estimate a maximum water content of 9 molecules per base or a 20% volume.

Table 2: Characterization parameters of the surfactant-DNA complexes obtained from open DNA gel particles, method 1.

Complexes	from 1D data	
	d (nm)	a (nm)
CTAB-DNA	5.47 ± 0.05	6.54 ± 0.05
MTAB-DNA	4.92 ± 0.05	5.68 ± 0.05
ALA-DNA	4.22 ± 0.05	4.87 ± 0.05
LAM-DNA	4.69 ± 0.05	5.41 ± 0.05

Studying in more detail the process of preparation by method 3, it was observed that the complex is forming only on the interface. In Figure 5, an example of the SAXS measurements at a different level in the capillary is presented. At the beginning of the contact of the two samples, a very thin layer is observed. Visually, with time, the film gets thicker-and-thicker, but the structure remains the same as judged from the SAXS scattering curves. The speed of this process depends on the surfactant and DNA concentrations. As it can be observed in the capillary, the interaction of DNA and MTAB is very fast. After half an hour at the bottom (DNA solution) and the top (MTAB solution) of the capillary, no peaks were observed in SAXS measurements. Although there should be some depletion of surfactant and DNA at each side of the film, we were not able to quantify it. The complex was formed only at the interface of the two solutions in a very thin layer, and this film is stable. This behavior of the complex formation in capillary was also observed for the other surfactant-DNA complexes. In the film structures, the orientation of DNA domains should be parallel to the interface and this orientation is better defined in GISAXS measurements.

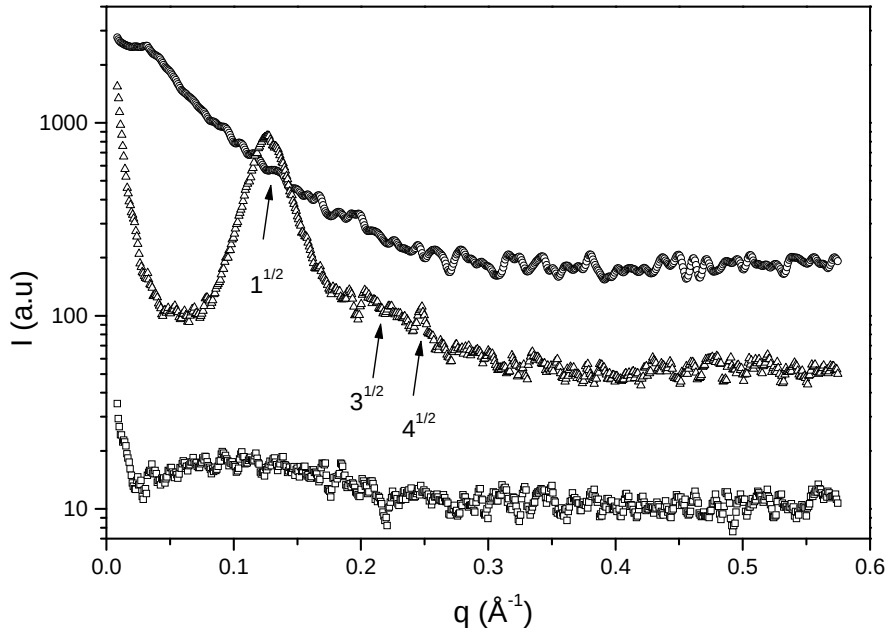

Figure 5: SAXS spectra for the MTAB-DNA film obtained using the method 3 (in capillary) and measurements at different levels. From bottom to top, measurement of the MTAB solution (□), MTAB-DNA complex (Δ) and DNA solution (○), respectively. The curves have been smoothed by adjacent averaging of 5 points. The small arrows show the approximate position of the hexagonal lattice peaks.

3.2.2. GISAXS Studies

It is well known that cationic surfactant-DNA complexes form liquid crystals[1, 20, 33] However, conditions for the formation of such structures are not sufficiently fully covered yet. Due to the low scattering volume obtained of thin films for SAXS analysis, we propose GISAXS measurements in order to characterize the surfactant-DNA complexes obtained using method 2 (dry film by spraying method) and compared with those obtained using method 1 (opening DNA gel particle). GISAXS is the method which was used in the last years for characterization of thin films and the previously difficult to interpret patterns of SAXS and GISAXS nowadays are relatively straightforward.[34,35] Therefore by GISAXS we investigate our complexes to get a better understanding of the formed nanostructure.

Figure 6 shows the representative GISAXS spectra for the different surfactant-DNA complexes obtained using both preparation methods.

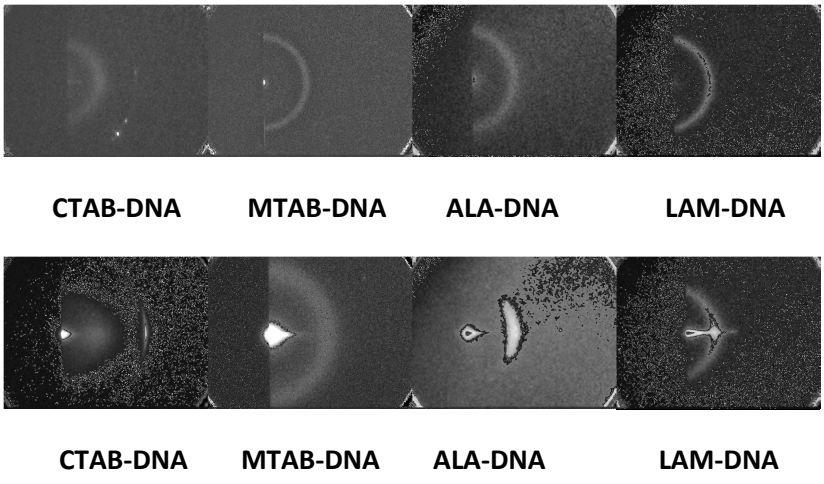

Figure 6: 2D GISAXS spectra of the corresponding surfactant-DNA complexes obtained using method 1 (opening DNA gel particle) - (A) and method 2 (dry film by spraying method) - (B).

Figure 6A shows the 2D GISAXS spectra of the surfactant-DNA complexes corresponding to the films obtained using method 1 (opening the DNA gel particles). In row ***A***, strong signal can be observed at different *q* values according to the surfactant used. These *q* values coincide with the ones detected using

1D detector (see values in Table 2). The existence of a diffuse ring on these spectra makes difficult to distinguish the second peak of the hexagonal arrangement visible for some samples using the 1D detector. As the rings are broad, it is evident that the film structure is powder-like with some short range order. However, in case of surfactant-DNA complexes obtained from films using method 2 (dry film by spraying method), an orientation can be observed for all surfactant-DNA complexes except for MTAB-DNA complexes (see Figure 6B). This orientation in the pattern, suggest a parallel orientation, that is, a hexagonal packing of cylinders on the surface. This clearly was observed for ALA-DNA sample where, azimuthal plots at the *q* of the maximum showed that weak peaks were present at $\theta = \pm 60^{o}$. In the pattern of this picture (2D spectra of ALA-DNA from Figure 6) shows spots exhibiting the six-fold symmetry (see Supporting Information Figure 2S) additional peaks at $\pm 25^{o}$ are also present in the hexagonal arrangement according to simulation (dashed curve in Figure 2S). The presence of spots instead of rings in the pattern is undoubtedly a sign for a long range order and substrate induces orientation. This order of orientation cannot be seen in the surfactant-DNA complexes obtained using method 1 (opening DNA gel particles), suggesting the which should be due to the thickness of the film, which in case of the method 2 (dry film by spraying method) is thinner and also the volume of the two solutions is fixed. This effect was observed in earlier studies and was mentioned that the film thickness can favor a parallel (commensurate) or perpendicular (incommensurate) orientation.[36] Another explanation would be, for example, the incomplete complexation of the surfactant-DNA complexes. The diffuse scattering in 2D becomes better defined for the samples prepared using method 2 (dry film by spraying method). The relative weakness of the spots (Figure 6B) suggests that a lamellar phase can be predominant in comparison to the hexagonal structure. A diffuse ring in GISAXS indicates a lack of long-range and orientation order. Although this scattering pattern could be interpreted as a cylindrical-type microstructure, the possibility of non-oriented lamellar phase cannot be excluded. From the observed pattern can be deduced that the surfactant-DNA complexes contain cylinders while the lattice parameter of the hexagonal packing was a few nanometer. The characterization parameters of the studied complexes from 2D measurements are summarized in Table 3.

Table 3: Characterization parameters of the surfactant-DNA complexes from 2D measurements

Complexes	Method 1		Method 2	
	d (nm)	a (nm)	d (nm)	a (nm)
CTAB-DNA	5.24 ± 0.05	6.05 ± 0.05	5.24 ± 0.05	6.05 ± 0.05
MTAB-DNA	4.55 ± 0.05	5.25 ± 0.05	3.27 ± 0.05	3.78 ± 0.05
ALA-DNA	3.90 ± 0.05	4.50 ± 0.05	4.00 ± 0.05	4.62 ± 0.05
LAM-DNA	4.65 ± 0.05	5.34 ± 0.05	4.49 ± 0.05	5.18 ± 0.05

The surfactant-DNA complexes prepared by different methods are formed due to the strong electrostatic attraction between the negatively charged DNA and the positive surfactant aggregates, and according to the X-ray measurements show close-packed nanostructures. The fact that MTAB and CTAB forms elongated micelles (ellipsoid like) in the vicinity of DNA[37,38] favors the formation of the complex. It is highly probable that with increasing the size of the head group, like in the case of ALA and LAM surfactants, the micelles formed in the corresponding surfactant-DNA complexes (ALA-DNA, LAM-DNA) can have a smaller hydrophobic core and a large hydrophilic domain which allows for stronger deformation of the micelles. A deeper analysis of the data indicates the presence of a stronger interaction between the cationic surfactant and DNA. For all of the studied complexes, a hexagonal packing was observed. Potential nanostructures of the hexagonal packing of the studied surfactant-DNA complexes are shown in Figure 7. For the films obtained using the method 1 (opening the DNA gel particles) and let to dry on a glass surface (Figure 7A) the nanostructure of the surfactant-DNA complex would present a hexagonal packing. In the unit cell of the 2D hexagonal structure, there is a central cylindrical surfactant aggregate (CTAB, MTAB, ALA or LAM micelle) that is surrounded by DNA helices. The surfactant micelles are hexagonally oriented around the DNA molecules in different arrangements (see Figure 7B and C).

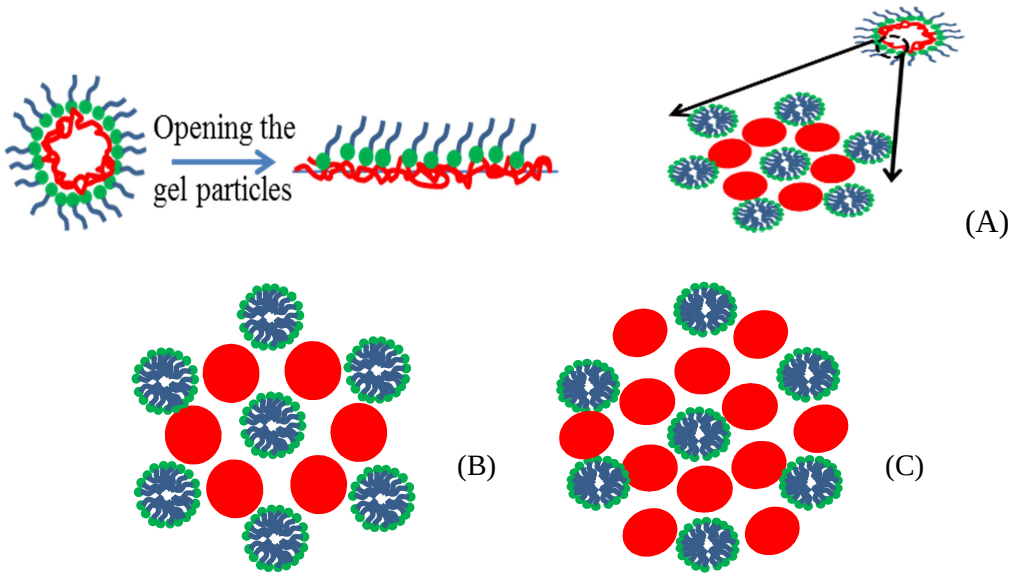

Figure 7: Schematic representation of the surfactant-DNA nanostructures: (A) Hexagonal packing, (B) 2:1 packing arrangement and (C) 3:1 packing arrangement. The red circles correspond to the DNA helices and the blue-green micelles for the surfactant cylinders. The (B) and (C) structures were proposed for CTAB-DNA complexes by Leal at al.[39]

In order to have a better general view on the composition of the surfactant-DNA complex on the films obtained using the method 1 additional Elemental Analysis of the dry films in the form of powder was carried out.

Table 4: Percentage of carbon and nitrogen content and the calculated number of surfactant molecules per one base of DNA segment.

	C %	N %	C/N	Surfactant/Base molar ratio
DNA	29.7	12.99	2.29	-
CTAB	62.65	3.84	16.32	-
MTAB	62.65	3.85	16.27	-
ALA	52.05	16.87	3.09	-
LAM	55.95	13.74	4.07	-
CTAB-DNA	52.25	10.10	5.17	**1.47**
MTAB-DNA	52.66	10.10	5.21	**1.78**
ALA-DNA	45.50	16.50	2.76	**2.18**
LAM-DNA	50.54	14.63	3.46	**1.86**

According to the experimental results and using the carbon/nitrogen ratio, we can calculate the number of surfactant molecules per DNA base (Table 4). For this calculation, we consider for each DNA segment four bases (guanine:cytosine:adenine:thymine). Our results suggest that each DNA base is surrounded with more than one surfactant molecule.

From these results, we can give a possible explanation of mutual arrangement of DNA helices and cationic surfactants in the complexes. Taking into account the different packing arrangements for electroneutral complexes as constituted by DNA helices and CTAB cylinders in 6-fold symmetry arrangements (helix:cylinder ratios 2:1, 3:1 and 5:1) proposed by Leal et al.[39] our calculations can be summarized as follows. We have used a value of 1.72 Å per DNA base and taking into account the hydrophobic length of the surfactants to form cylinders. For the surfactants, the used length and volume values are summarized in Table 5 together with the theoretically calculated surfactant/base molar ratio for the different DNA helices/surfactant arrangements

Table 5: Characteristic parameters of the studied cationic surfactants

	Hydrophobic length / Å	Hydrophobic volume / Å^3	Surfactant/Base molar ratio for different arrangements		
			2:1	**3:1**	**5:1**
CTAB	21.7[38]	460	2.73	1.82	1.09
MTAB	19.2	406	2.42	1.61	0.97
ALA	16.7	352	2.12	1.41	0.85
LAM	15.0[26]	325	1.84	1.23	0.74

For CTAB-DNA and MTAB-DNA complexes the experimental Surfactant/Base molar ratios are 1.47 and 1.78 respectively, close to those expected for a 3:1 arrangement, which agrees with previous results[39,40]. However, for ALA-DNA and LAM-DNA complexes the experimental values are significantly bigger, 2.18 and 1.86 respectively, which are close to that expected for the 2:1 arrangement. The preferred structure of the complexes seems to be strongly related to the hydrophilic part of the cationic surfactants. Surprisingly, the smaller the hydrophilic head of the surfactant, the bigger the critical packing cell parameter of the complex while in the lamellar arrangement obtained for the single surfactant powders, the CTAB and MTAB show smaller cell sizes than ALA and LAM. In the case of ALA and LAM, the head-group is larger and also ALA has one more positive charge. The lamellar packing of surfactant aggregates, as it has been seen from X-ray measurement, shows 8.8-7.2 Å larger *d* values compared with CTAB. This difference in the complex is in the other sense, producing 12-8 Å bigger *d* for the CTAB complexes than for ALA and LAM. Therefore, it is clear that the packing arrangement has to be different. The nanostructure of the complexes strongly suggests a hexagonal packing. From the present results, it appears that the specific head group structure of ALA and LAM allows for a more compact packing because the hydrophilic corona can extend its influence much further away than in the case of CTAB. This is due to the longer and flexible nature of the head group, which allows for reducing the repulsive interactions from neighboring DNA helices in a more effective way. In the case of CTAB, a distortion/expansion of the cationic surfactant cylinder is needed to increase the surfactant-DNA interaction, and this should also result in an increase of conformational disorder of the alkyl chains[40]. These observations clarify the clear correlation between DNA release and the packing parameters, the shorter the lattice parameter, the stronger the interaction and the smaller the release[27].

These studied simple preparation methods (method 1 for gel particles and method 2 and 3 for films) allow for applications that take advantage of the hydrogel, but it can also be applied to biomedical applications such as controlled drug release for multiple drugs. More applications in other fields are also being explored. One possible application of these films is to use them as drug delivery vehicles by loading the complex with active molecules or simply by the delivery of its constituent molecules. The formation of stable surfactant-DNA complexes will increase the application of these systems. These surfactant-DNA complexes notably expand the potential for real-world applications, including cell therapy and other medicinal applications.

4 Conclusions

The cationic-surfactant complexes show strong electrostatic interaction and in-plane (surface/interface) orientation. In our work, we have discussed in detail the structural behavior of surfactant-DNA complexes on films obtained using different preparation methods. We can conclude that the particles showed a clear evidence of an ordered nanostructure of the surfactant-DNA complexes which should be involved in the stabilization of the obtained particles. The nanostructure of the complexes strongly suggests a hexagonal packing. The GISAXS measurements showed that when the film is formed by method 2 there is a parallel orientation on the surface, which is a similar situation to the interface between DNA and surfactant solutions in the processes occurring in methods 1 and 3.

The thickness of the surfactant hydrophobic domain increases with increasing alkyl chain length, however, the change induced by the head group structure is stronger in the liquid crystal behavior of cationic surfactants than that accounted only by total chain length. The different surfactants show different hydrophobic chain conformation, with that of the quaternary ammonia being tilted and that of the arginine derivatives correspondingly straight. Also, the arginine derivatives have one or two positive charges to provide an electrostatic interaction, in addition to multiple hydrogen bonding donor and acceptor possibilities.

The ALA-DNA and LAM-DNA complexes show 2:1 packing arrangement as the ALA and LAM surfactants have bigger and more flexible hydrophilic head group compared to CTAB and MTAB surfactants they can accommodate this arrangement that is more distorted than 3:1. For CTAB-DNA and MTAB-DNA complexes 3:1 DNA helices/surfactant cylinder ratio is more favorable which should also result from the increased conformation disorder of the alkyl chain.

The present results may allow future applications of these complexes for improved biocompatibility, stability and nanostructure in medicinal and pharmaceutical applications.

5 Acknowledgements

Imma Carrera is acknowledged for technical assistance. Jaume Caelles from the IQAC SAXS-WAXS Service and the Microanalysis Service from IQAC are acknowledged for measurements. This work was supported by CSIC through a JAE-DOC2010-097 contract co-financed by FSE 2007-2013. Financial support by CTQ2010-14897 from MINECO (Spain) and 2009SGR1331 from Generalitat de Catalunya is

acknowledged. M.C. Morán acknowledges the support of the MICINN (Ramon y Cajal contract RyC 2009-04683).

6 Notes and references

[1] Rädler J. O., Koltover I., Salditt T., Safinya C. R., Structure of DNA-cationic liposome complexes: DNA intercalation in multilamellar membranes in distinct interhelical packing regimes, *Science* **1997**, 275, 810-814.

[2] Templeton N. S., Lasic D. D., Frederik P. M., Strey H. H., Roberts D. D., Pavlakis G. N., Improved DNA: Liposome complexes for increased systematic delivery and gene expression, *Nature Biotech.*, **1997**, 15, 647-652.

[3] Martin B., Aissaoui A., Sainlos M., Oudrhiri N., Hauchecorne M., Vigneron J. P., Lehn J. M., Lehn P., Advances in cationic lipid-mediated gene delivery, *Gene Ther. Mol. Biol.*, **2003**, 7, 273-289.

[4]Caracciolo G., Sciubba F., Caminiti R., Effect of hydration on the structure of caveolae membranes, *App. Phys. Lett.* **2009**, 94, 153901-1-153901-3.

[5] Dias R. S., Lindman B., Miguel M. G., Compaction and decompaction of DNA in the presence of Catanionic amphiphile mixtures, *J. Phys. Chem. B.*, **2002**, 106, 12608-12612

[6] Xu Y., Hui S. W., Federic P., Szoka F. C., Jr., Physicochemical characterization and purification of cationic lipoplexes, *Biophys. J.*, **1999**, 77, 341-355.

[7] Montigny W. J., Houchens C. R., Illenye S., Gilbert J., Coonrod E., Chang Y. C., Heintz N. H., Condensation by DNA looping facilitates transfer of large DNA molecules into mammalian cells, *Nucleic Acids Res.*, **2001**, 29, 1982-1988.

[8] Duguid J. G., Li C., Shi M., Logan M. J., Alila H., Rolland A., Tomlinson E., Sparrow J. T., Smith L. C., A physicochemical approach for predicting the effectiveness of peptide-based gene delivery systems for use in plasmid-based gene therapy, *Biophys. J.*, **1998**, 74, 2802-2814.

[9] Gaweda S., Morán M. C., Pais A. A. C. C., Dias R. S., Schillen K., Lindman B. and Miguel M. G., Cationic agents for DNA compaction *J. Colloid Interface Sci., 2008*, 323, 75-83.

[10] Pinto M. F., Morán M. C., Miguel M. G., Lindman B., Jurado A. S., Pais A. A. C. C., Controlling the Morphology in DNA Condensation and Precipitation, *Biomacromolecules*, **2009**, 10, 1319-1323.

[11] Paulsson M., Edsman K., Controlled drug release from gels using surfactants aggregates. Part II.: vesicles formed from mixtures of amphiphilic drugs and oppositely charged surfactants. *Pharm. Res.*, **2001**, 18:1586-1592.

[12] Pérez L., Pinazo A., Gracia M. T., Lozano M., Manresa A., Angelet M., Vinardell M. P., Mitjans M., Pons R., Cationic surfactants from lysine: Synthesis, micellization and biological evaluation, *Eur. J. Med. Chem.*, **2009**, 44, 18884-1892.

[13] Scholer N., Olbrich C., Tabatt K., Muller R.H., Hahn H., Liesenfeld O., Surfactant, but not the size of solid lipid nanoparticles influences viability and cytokine production of macrophages, *Int. J. Pharm.*, **2001**, 221, 57-67.

[14] Lozano N., Pérez L, Pons R., Pinazo A., Diacyl glycerol arginine-based surfactants: biological and physicochemical properties of catanionic formulations, *Amino Acids*, **2011**, 40, 721-729.

[15] Bouxsein N. F., McAllister C. S., Ewert K. K., Samuel C. E., Safinya C. R., Structure and gene silencing activities of monovalent and pentavalent cationic lipid vectors complexed with siRNA, *Biochemistry*, **2007**, 46, 4785-4792

[16] Gawrisch K., Parsegian V. A., Hajduk D. A., Tate M. W., Gruner S. M., Fuller N. L., Rand R. P., Energetics of a hexagonal–lamellar–hexagonal-phase transition sequence in dioleoylphosphatidylethanolamine membranes, *Biochemistry*, **1992**, 31, 2856-2864

[17] Ijiro K., Okahata Y., A DNA-lipid complex soluble in organic solvents, *J. of the Chem. Soc.-Chem. Commun*., **1992**, 1339-1341

[18] Morán M. C., Miguel M. G., Lindman B., Surfactant-DNA gel particles: Formation and release characteristics, *Biomacromolecules*, **2007**, *8* (12), pp 3886–3892.

[19] Saminathan M., Thomas T., Shirahata A., Pillai C. K. S., Thomas T. J., Polyamine structural effects on the induction and stabilization of liquid crystalline DNA: Potential applications to DNA packing, gene therapy and polyamine therapeutics, *Nucleic Acids Res.*, **2002**, 30, 3722-3731.

[20] Koltover I., Salditt T., Radler J. O., Safinya C. R., An Inverted Hexagonal Phase of Cationic Liposome-DNA Complexes Related to DNA Release and Delivery, *Science*, **1998**, 281, 78-81.

[21] Bloomfield V. A., DNA condensation, *Curr. Opin. Struct. Biol.* **1996**, 6, 334-341.

[22] Blessing T., Remy J. S., Behr J. P., Monomolecular collapse of plasmid DNA into stable virus-like particles, *Proc. Natl. Acad. Sci., U.S.S.*, **1998**, 95, 1427-1431.

[23] Sambrook J., Fritsch, E. F.; Maniatis, *T. Molecular Cloning: a laboratory manual*; Cold Spring Harbor Laboratory Press, New York, USA, **1989**; Vol. 3, App. C.1.

[24] Infante M. R., Dominguez J. G., Erra P., Julia M. R., Prats M., Surface active molecules: Preparation and properties of long chain N(α)-acyl-L-α-amino-ω-guanidine alkyl acid derivatives, *Int. J. Cosmet. Sci.*, **1984**, 6, 275-282.

[25] Clapés P., Morán M. C., Infante M. R., Enzymatic synthesis of arginine-based cationic surfactants, *Biotechnol. Bioenerg.* **1999**, 63, 333-343.

[26] Pérez L., Pinazo A., Infante M. R., Pons R., Investigation of the micellization process of single and gemini surfactants from arginine by SAXS, NMR self-diffusion, and light scattering, *J. Phys. Chem. B*, **2007**, 111, 11379.

[27] Morán M. C., Infante M. R., Miguel M. G., Lindman B., Pons R., Novel Biocompatible DNA Gel Particles, *Langmuir*, **2010**, 26 (13), 10606-10613.

[28] Dasgaputa A., Das P. K., Dias R. S., Miguel M. G., Lindman B., Jadhav V. M., Gnanamani M., Maiti S., Effect of Headgroup on DNA-Cationic surfactant interactions, J. Phys. Chem B., 2007, 111, 8502-8508.

[29] Dietrich Demus, Lothar Richter –*Texture of Liquid Crystals*, VEB Deutscher Verlag für Grundstoffindustrie, Leipzig, 2nd edition, **1978**

[30] Small M. D. Handbook *of Lipid Research 4*, The Physical Chemistry of Lipids, From Alkanes to Phospholipids, Plenum Press, new York and London, **1986**

[31] Paradies H. H. and Clancy S. F. Crystalline polymorphism of cetyltrimethylammonium bromide and distearyldimethylammonium (DSDMA) compounds. A comparison of the hydrated DSDMA-Chloride, DSDMA-S-(+)-Lactate and DSDMA-Pyruvate systems., *The Rigaku Journal*, Vol 17, No.2, **2000.**

[32] Krishnaswamy R., Pabst G., Rappolt M., Raghunathan V. A., Sood A. K., Structure of DNA-CTAB-hexanol complexes, *Phys. Rev. E.*, **2006**, 73, 31904-31908

[33] Leal C., Bilalov A., Lindman B., *J. Phys. Chem. B.*, **2009**, 113, 9909-9914

[34] Tate M. P., Urade V. N., Kowalski J. D., Wei Ta-chen, Hamilton B. D., Eggiman B. W., Willhouse H. W., Simulation and Interpretation of 2D Diffraction Patterns from Self-Assembled Nanostructured Films at Arbitrary Angles of Incidence: From Grazing Incidence (Above the Critical Angle) to Transmission Perpendicular to the Substrate, *J. Phys. Chem B*, **2006,** 110, 9882-9892.

[35] Dunphy D. R., Alam T. M., Tate M. P., Hillhouse H. W., Smarsly B., Collord A. D., Carnes E., Baca H. K., Kohn R., Sprung M., Wang J., Brinker C. J., Characterization of Lipid-Templated Silica and Hybred Thin Film Mesophases by Grazing Incidence Small-Angle X-RAY Scattering, *Langmuir*, **2009**, 25, 9500-9509.

[36] Langa S., Christopher M., Cartensen J., Tiginyanu I. M., Föll H., Single crystalline 2D porous arrays obtained by self-organization in n-InP, *Phys.stat.sol.*, 197, 77-82, **2003**.

[37] Dias R. S., Lindman B., Miguel M. G., Interactions between DNA and surfactants, *Prog. In Colloid and Polym. Sci.*, **2001**, 118, 163-167.

[38] Ghirlando R., Wachtel E. J., Arad T., Minsky A., DNA Packing Induced by Micellar Aggregates: A Novel in Vitro DNA Condensation System, *Biochemistry*, **1992**, 31, 7110-7119.

[39] Leal C., Wadsö L., Olofsson G., Miguel M.G., Wennerström H., The Hydration of a DNA-Amphiphile Complex, *J. Phys. Chem B.*, **2004**, 108, 3044-3050.

[40] Leal C., Topgaard D., Martin R. W., Wennerström H., NMR Studies of Molecular Mobility in a DNA-Amphiphile Complex, *J. Phys. Chem. B*, **2004**, 108, 15392-15397.

Electronic supplementary information (ESI)

The nanostructure of surfactant-DNA complexes with different arrangements

Amalia Mezei[1], Ramon Pons[1*], M. Carmen Morán[2]

[1] Departament de Tecnología Química y de Tensioactius, Institut de Química Avançada de Catalunya, IQAC-CSIC, c. Jordi Girona 18-26, 08034 Barcelona, Spain

[2]Departament de Fisiologia, Facultat de Farmàcia, Universitat de Barcelona, Avda. Joan XXIII, 08028 Barcelona, Spain

[*] Corresponding author email: *ramon.pons@iqac.csic.es*

Figure 1S – Sample preparation methods

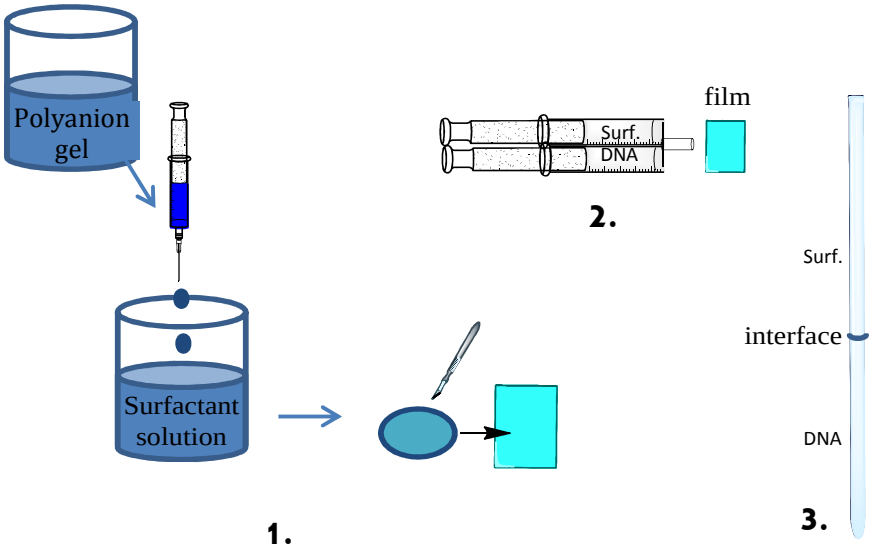

Figure 1S: Sample preparation technics: **Method 1**- Particle formation; **Method 2**- Film formation by spraying; **Method 3**- Film formation in capillary.

Figure 2S – Azimuth spectra of ALA-DNA

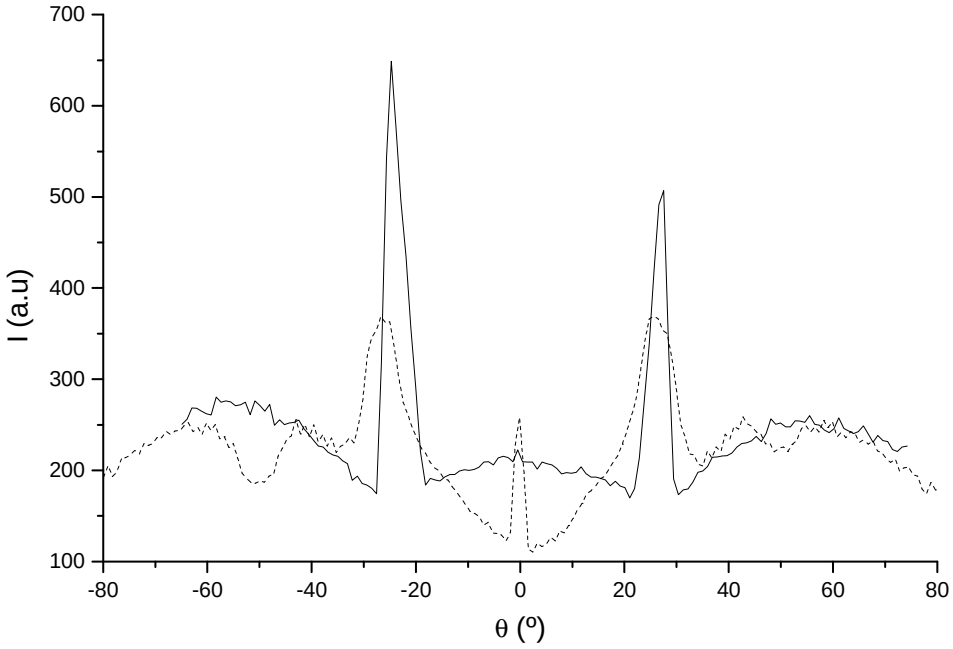

Figure 2S: Azimuthal scattered intensity at q=1.61 nm^{-1} of ALA-DNA complex, the full line corresponds to the sprayed film and the dashed line is the simulated spectra for 2:1 arrangement.